
This is an electronic reprint of the original article.
This reprint *may differ* from the original in pagination and typographic detail.

Author(s): Smallcombe, J.; P.J.Davies; C.J.Barton; D.G.Jenkins; L.L.Andersson; P.A.Butler; D.M.Cox; R.-D.Herzberg; A.Mistry; E.Parr; Grahn, Tuomas; Greenlees, Paul; Hauschild, Karl; Herzan, Andrej; Jakobsson, Ulrika; Jones, Peter; Julin, Rauno; Juutinen, Sakari; Ketelhut, Steffen; Leino, Matti; Lopez-Martens, Araceli; Nieminen, Päivi; Pakarinen, Janne; Papadakis, Philippos; Peura, Pauli; Rahkila, Panu; Rinta-Antila, Sami; Ruotsalainen, Panu; Sandzelius, Mikael; Sarén, Jan; Scholey, Catherine; Sorri, Juha

Title: Experimental investigation of the O^*_2 band in ^{154}Sm as a β -vibrational band

Year: 2014

Version:

Please cite the original version:

Smallcombe, J., P.J.Davies, C.J.Barton, D.G.Jenkins, L.L.Andersson, P.A.Butler, D.M.Cox, R.-D.Herzberg, A.Mistry, E.Parr, Grahn, Tuomas, Greenlees, Paul, Hauschild, Karl, Herzan, Andrej, Jakobsson, Ulrika, Jones, Peter, Julin, Rauno, Juutinen, Sakari, Ketelhut, Steffen, Leino, Matti, Lopez-Martens, Araceli, Nieminen, Päivi, Pakarinen, Janne, Papadakis, Philippos, Peura, Pauli, Rahkila, Panu, Rinta-Antila, Sami, Ruotsalainen, Panu, Sandzelius, Mikael, Sarén, Jan, Scholey, Catherine, Sorri, Juha, Uusitalo, Juha. (2014). Experimental investigation of the O^*_2 band in ^{154}Sm as a β -vibrational band. *Physics Letters B*, 732(May), 161-166.
<https://doi.org/10.1016/j.physletb.2014.03.034>

All material supplied via JYX is protected by copyright and other intellectual property rights, and duplication or sale of all or part of any of the repository collections is not permitted, except that material may be duplicated by you for your research use or educational purposes in electronic or print form. You must obtain permission for any other use. Electronic or print copies may not be offered, whether for sale or otherwise to anyone who is not an authorised user.



Experimental investigation of the 0_2^+ band in ^{154}Sm as a β -vibrational band



J. Smallcombe^{a,*}, P.J. Davies^a, C.J. Barton^a, D.G. Jenkins^a, L.L. Andersson^b, P.A. Butler^b, D.M. Cox^b, R.-D. Herzberg^b, A. Mistry^b, E. Parr^b, T. Grahn^c, P.T. Greenlees^c, K. Hauschild^{c,d}, A. Herzan^c, U. Jakobsson^c, P. Jones^c, R. Julin^c, S. Juutinen^c, S. Ketelhut^c, M. Leino^c, A. Lopez-Martens^{c,d}, P. Nieminen^c, J. Pakarinen^c, P. Papadakis^{c,b}, P. Peura^c, P. Rahkila^c, S. Rinta-Antila^c, P. Ruotsalainen^c, M. Sandzelius^c, J. Sarén^c, C. Scholey^c, J. Sorri^c, J. Uusitalo^c

^a Department of Physics, University of York, Heslington, York YO10 5DD, United Kingdom

^b Oliver Lodge Laboratory, University of Liverpool, Liverpool L69 9ZE, United Kingdom

^c Department of Physics, University of Jyväskylä, FI-40014, Finland

^d CSNSM-IN2P3-CNRS, Université Paris-Sud, 91406 Orsay, France

ARTICLE INFO

Article history:

Received 10 January 2014

Received in revised form 20 February 2014

Accepted 18 March 2014

Available online 21 March 2014

Editor: D.F. Geesaman

Keywords:

Internal conversion electrons

Gamma ray

Spectroscopy

Electric monopole

Collective models

Rare-earth

ABSTRACT

A study of ^{154}Sm through γ -ray and internal conversion electron coincidence measurements was performed using the Silicon And Germanium spectrometer (SAGE). An upper limit for the $\rho^2(E0; 2_2^+ \rightarrow 2_1^+)$ and measurement of the $\rho^2(E0; 4_2^+ \rightarrow 4_1^+)$ monopole transitions strengths were determined. The extracted transition strength for each is significantly lower than that predicted by either the Bohr and Mottelson β -vibration description or the interacting boson model. Hence, the long standing interpretation of these states as a collective band built on the 0_2^+ state, which is conventionally assigned as a Bohr and Mottelson β vibration is questionable.

© 2014 The Authors. Published by Elsevier B.V. This is an open access article under the CC BY license (<http://creativecommons.org/licenses/by/3.0/>). Funded by SCOAP³.

1. Introduction

The first excited 0^+ states in the vast majority of even–even rare-earth nuclides have long been interpreted as collective excitations. This is due, in part, to these states being observed below the pairing gap. Collective behaviour in nuclei that are known to have significant quadrupole deformation can be described by a geometric model of an axially symmetric rotor. The most successful and long-standing theoretical description of such collective behaviour involve solutions to the Bohr and Mottelson Hamiltonian [1]. Solutions to this Hamiltonian show that collective excitation modes may arise from shape oscillations parallel to (β vibration) or perpendicular to (γ vibration) the symmetry axis. A significant amount of experimental evidence exists for γ vibrations, and typically the first rotational structure identified as being built

on a $K = 2$ state is labelled as the γ -band. Hence, it is common practise to label the first excited 0^+ state as a β vibration and the rotational structure built upon this state as a β -band. However, a significant amount of theoretical [2–5] and experimental [6–11] work has questioned this interpretation.

The historical approach of identifying these β -bands simply by the energy spacing of the 0_2^+ , 2_2^+ and 4_2^+ states is not sufficiently rigorous [2]. This method belies the evidence provided by modern measurements such as $B(E2)$ and $\rho^2(E0)$ strengths. An enhanced decay strength should be seen in the case of $E0$ decays from a β -band to the ground state band (GSB). These $E0$ transition rates can be related to $B(E2)$ values by [12,13]:

$$\begin{aligned} \rho^2(E0; n_\beta = 1 \rightarrow n_\beta = 0) &= \frac{9}{8\pi^2} Z^2 \beta_0^4 \frac{E(2_1^+)}{E(0_1^+)} \\ &= \frac{B(E2; 0_1^+ \rightarrow 2_\beta^+) 4\beta_0^2}{e^2 r_0^4 A^{4/3}}, \end{aligned} \quad (1)$$

* Corresponding author.

E-mail address: james.smallcombe@outlook.com (J. Smallcombe).

where n_β denotes the number of β -vibration quanta of a state, β_0 is the static quadrupole deformation of the ground state and r_0 is 1.3 fm. Typical values of $B(E2)$ for β -vibrator candidates provide values of $\rho^2(E0)$ in the region of $85\text{--}230 \cdot 10^{-3}$ [2].¹ There is no angular momentum dependence in Eq. (1), and therefore all $\rho^2(E0; I_i^+ \rightarrow I_f^+)$ values for a given isotope should be of a similar magnitude. A compilation of $\rho^2(E0)$ measurements [13] showed that, with the exception of ^{162}Er , $\rho^2(E0) \approx 90 \cdot 10^{-3}$ represents an upper limit for $I_i^+ \rightarrow I_f^+$ measurements in the rare-earth nuclides. This suggests that few of the identified 0_2^+ bands are in fact pure β vibrations.

Notably, maximum $E0$ strengths close to samarium are found for the $N = 90$ isotones, where $\rho^2(E0; 0_2^+ \rightarrow 0_1^+) \approx 80\text{--}90 \cdot 10^{-3}$, with a significant reduction in the adjacent isotopes of lower mass [14]. Such localised increases in $E0$ strength are also observed elsewhere across the nuclear landscape. Theoretical efforts to explain these increases have predominantly employed the Interacting Boson Model (IBM), incorporating s and d bosons [15,16] and more recently s , d , and g bosons [16].

Interpretation of the experimental and theoretical results is a matter of debate. Work by Casten et al. [17] suggests that this is a case of phase transition, where the $N = 90$ isotones represent a midpoint between nuclides with a spherical and deformed ground state. An alternative interpretation by Garrett et al. [18] suggests that these nuclei may represent a shape coexistence phenomenon. Wood et al. [13] demonstrate that for such coexisting states, simple two-state mixing calculations can account for a significant increase in $E0$ strength. However, it is clear that the lack of experimental information on $E0$ strengths in these nuclei, specifically for $N > 90$ in the rare-earth region, is hampering the understanding of their low-lying structure.

The isotope ^{154}Sm lies at the heart of the rare-earth region, has a large ground-state quadrupole deformation, and neighbours the $N = 90$ isotones. As such, it is an ideal candidate to be described by β vibrations in the Bohr and Mottelson Hamiltonian. Furthermore, measuring the strength of $E0$ transitions beyond $N = 90$ will provide a test of IBM calculations in the rare-earth nuclides. Such measurements should provide further information on the ongoing debate between shape-coexistence and phase-transitions descriptions of the $N = 90$ isotones.

In this letter, measurements of $\rho^2(E0; I_2^+ \rightarrow I_1^+)$ strengths in ^{154}Sm using the newly commissioned Silicon And GERmanium (SAGE) spectrometer [19,20] are reported. A previous attempt to measure $E0$ strengths in ^{154}Sm reported values of $\rho^2(E0; 0_2^+ \rightarrow 0_1^+) = 96(42) \cdot 10^{-3}$ and $\rho^2(E0; 2_2^+ \rightarrow 2_1^+) < 6.3 \cdot 10^{-3}$ [21]. These values are inconsistent with the interpretation of a rotational band built on a β vibration. As the previous experiment was insufficiently sensitive to γ rays, it was not possible to separate $E0$ strength measurements of the $2_2^+ \rightarrow 2_1^+$ and $0_2^+ \rightarrow 0_1^+$ transitions, due to their similar energies. This article will present experimental details in Section 2, results in Section 3, and a discussion of these results in Section 4.

2. Experiment

The experiment employed the SAGE spectrometer at the University of Jyväskylä (JYFL) to make a simultaneous measurement of γ rays and conversion electrons resulting from the Coulomb excitation (CoulEx) of ^{154}Sm . This array consists of 34 High-Purity Germanium detectors (24 Clover and 10 EUROGAM Phase I detectors), from the JUROGAMII array, coupled to a highly segmented silicon detector located approximately 1 m upstream of the target

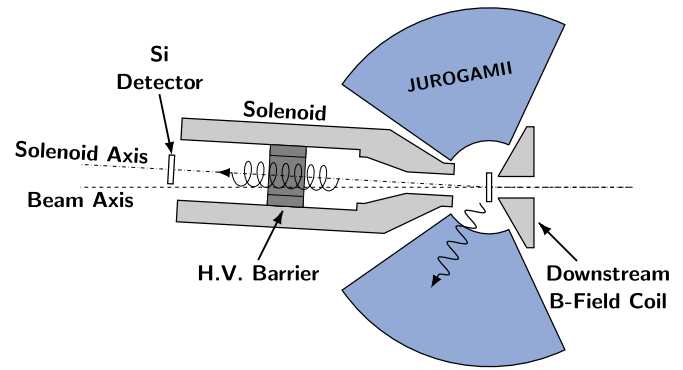


Fig. 1. (Colour online.) Cut-through illustration of the experimental geometry showing the relative locations of JUROGAMII and the silicon detector that comprise the SAGE spectrometer. The samarium target was situated at the focal-point of JUROGAMII. Solenoid coils downstream and upstream of the target create the field that transports electrons to the SAGE silicon detector. The axis of the upstream solenoid is 3.2° from the beam axis to permit passage of the beam beside the detector. A high-voltage potential barrier within the upstream solenoid suppresses δ -electrons.

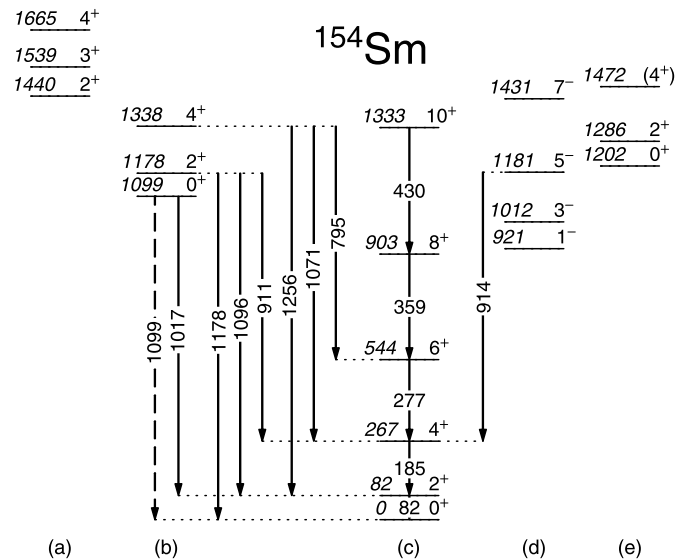


Fig. 2. Energy level diagram of the low-energy bands of ^{154}Sm . Levels are organised into the (a) $K=2$ " γ -band", (b) 0_2^+ band suggested as the " β -band", (c) ground state band, (d) first negative parity band and (e) 0_1^+ band. Level energies are given in keV, along with spins and their associated parities. Arrows denote selected transitions with energies given in keV, the dashed arrow is a pure $E0$ transition.

position, see Fig. 1. The Si detector is a 1-mm thick single-sided annular strip detector divided into 90 segments.

Conversion electrons resulting from the de-excitation of target nuclei are transported to the silicon detector by a solenoidal magnetic field. A high-voltage barrier is positioned between the target chamber and the silicon detector, suppressing the flux of δ -electrons resulting from the interaction of the beam and target. From calibration source data, SAGE has an efficiency, at 200 keV, of 9% for the detection of γ rays and 6% for the detection of conversion electrons.

States of interest in the 0_2^+ band of ^{154}Sm , shown in Fig. 2, were primarily populated by CoulEx using an ^{16}O beam at an energy of 65 MeV. The ^{154}Sm target, isotopically enriched to 99% and of areal density 1.5 mg/cm^2 , was mounted on the target wheel at the focal point of JUROGAMII. Data were recorded using the JYFL total data readout system [22], which individually digitises all detector channels without a common trigger. A fold-two requirement was

¹ All values of $\rho^2(E0)$ are presented in units of 10^{-3} by convention.

Table 1
Summary of experimentally measured ICCs.

Nuclide	I_i^π	I_f^π	E_γ (keV) ^a	E_K (keV) ^b	σL	$\alpha_{K,exp}$	Literature value ^{a,b}
¹⁵² Sm	2_2^+	4_1^+	562.9	516.1	E2	0.0069(34)	0.0078(1)
¹⁵² Sm	2_2^+	2_1^+	688.7	641.9	E0 + M1 + E2	0.0297(75)	0.0359(13)
¹⁶⁶ Yb	$8_{(3)}^+$	8_1^+	754.8	693.5	E0 + M1 + E2	0.0158(45)	0.017(3)
¹⁶⁶ Yb	$(6)_2^+$	6_1^+	814.5	753.2	M1	0.0069(28)	0.010(1)
¹⁵⁴ Sm	2_2^+	4_1^+	910.96	864.13	E2	0.0034(16)	0.00257(4)
¹⁵⁴ Sm	2_2^+	2_1^+	1095.86	1049.03	E0 + M1 + E2	$\leq 0.0067(6)$	–
¹⁵⁴ Sm	4_2^+	4_1^+	1070.98	1023.85	E0 + M1 + E2	$0.0079_{-0.0073}^{+0.0087}$	–

^a Values taken from the National Nuclear Data Center (NNDC) at Brookhaven National Lab (BNL).

^b Values from BrIcc tables [25].

placed on data written to disk, i.e. only data in which two or more channels triggered within 200 ns were recorded.

The beam energy of 65 MeV was chosen in order to maximise the population of the states of interest; this is sufficiently close to the combined Coulomb barrier height that a significant nuclear contribution to the reaction is anticipated. However, the experiment is insensitive to the means of excitation as no attempt is made to extract information from the population process. Cross sections for population of the 0_2^+ , 2_2^+ and 4_2^+ states by CoulEx were calculated to be 1.4, 7.2 and 1.3 mb respectively. Population of the 0_2^+ (1099 keV), 2_2^+ (1178 keV) and 4_2^+ (1338 keV) states were confirmed by observation of their respective transitions to the GSB in the γ -ray data. Transitions were also observed for the target contaminant ¹⁵²Sm and for the sub-barrier fusion-evaporation product ¹⁶⁶Yb. Data were collected for a total of 65 hours with an average beam current of 20 pA.

3. Results

Using the same requirement as the experimental trigger, $\gamma\gamma$ and γe^- coincidence events were constructed from individual detector events stored on disk. Coincident $\gamma\gamma$ pairs, which fell within a 60 ns time window, were added to a matrix of prompt events. A second matrix was constructed from coincident γe^- pairs for events in which the electron was detected between 100 ns before and 60 ns after the γ ray. These times encompass the observed genuine-coincidence timing peaks. Events which fell outside of these ranges, but within the 200 ns experimental trigger window, were added to background matrices. Background matrices were scaled according to the observed peak-to-total of timing spectra and subtracted from the prompt matrices to remove random coincidences. Subsequently, identical γ -ray gates were placed on each matrix to produce counterpart electron and γ -ray spectra, from which internal conversion coefficients (ICCs) were measured.

The conversion-electron sources ¹³³Ba and ²⁰⁷Bi were used to extract efficiencies for SAGE across the energy range of interest. A peak detection efficiency of 0.14% was measured for 1049 keV electrons, corresponding to ¹⁵⁴Sm $2_2^+ \rightarrow 2_1^+$ K-electrons. In order to account for data acquisition system differences between $\gamma\gamma$ and γe^- events (e.g. dead time, trigger response), the relative intensities of transition γ rays and electrons were normalised using the Normalised-Peak-to-Gamma (NPG) method [23]. The relative intensities of γ rays and electrons for known transitions are measured and an energy independent scaling constant, $C_{\gamma e^-}$, is determined from established ICCs. This normalisation was performed using 20 E2 transitions in the GSB of ¹⁵⁴Sm, ¹⁵²Sm and ¹⁶⁶Yb, all of which were clearly discernible in the data following γ -ray gating; an example spectrum is shown in Fig. 3. Subsequent ICCs are then given by:

$$\alpha_{exp} = \frac{N_{e^-} \epsilon_\gamma}{N_\gamma \epsilon_{e^-}} C_{\gamma e^-} W(\theta), \quad (2)$$

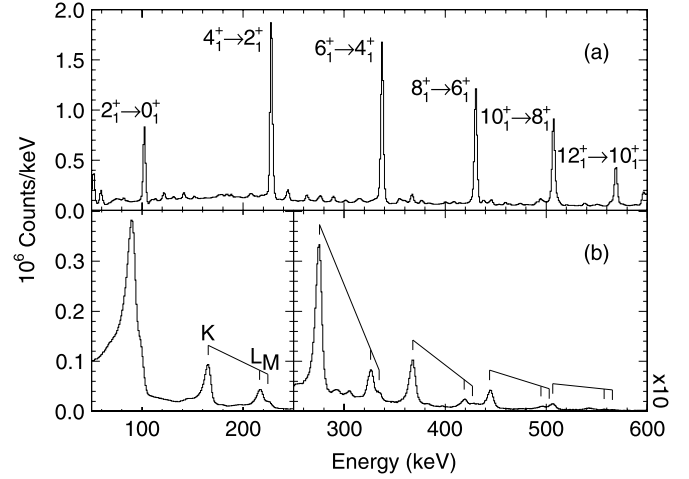


Fig. 3. Spectra showing the (a) γ rays and (b) electrons detected in SAGE, both following gating on yrast transitions of ¹⁶⁶Yb. The γ -rays peaks of ¹⁶⁶Yb are labelled and markers below indicate the K, L and M components of the corresponding electron peak. The right hand side of the electron spectrum has been magnified by a factor of 10 for greater clarity.

where N_γ and N_{e^-} are the peak counts of γ rays and electrons, respectively, and ϵ_γ and ϵ_{e^-} are the respective detector efficiencies. $W(\theta)$ is a factor which accounts for the effect of different angular correlations between $\gamma\gamma$ and γe^- . The effect was estimated to be less than 2%; this is smaller than the uncertainties on the other parameters and so $W(\theta)$ was taken to be 1, consistent with the work of Ref. [24].

ICCs were measured for known transitions from non-yrast states in ¹⁵⁴Sm, ¹⁵²Sm and ¹⁶⁶Yb. A summary of these results is presented in Table 1, along with literature values. These transitions from excited bands to the GSB lie in the energy range 500–1000 keV. Due to both the electron detection efficiency and the magnitude of ICCs decreasing with energy, the statistics of associated electron peaks were limited. This was coupled with a large statistical variance following background subtraction, resulting in large N_{e^-} errors. Hence, N_{e^-} measurements are taken at the 95% confidence limit, leading to large uncertainties on α_{exp} , within which consistency with previous measurements is achieved.

The γ -ray and electron fits for the $2_2^+ \rightarrow 4_1^+$ (911.0 keV) transition in ¹⁵⁴Sm, obtained by gating on the $4_1^+ \rightarrow 2_1^+$ (184.8 keV) γ ray, are shown in Fig. 4. The peak of the $5_1^- \rightarrow 4_1^+$ (914.4 keV) γ ray can be seen to overlap with the $2_2^+ \rightarrow 4_1^+$ γ ray. The $5_1^- \rightarrow 4_1^+$ γ -ray peak is significantly Doppler-broadened due to the short lifetime of the initial state. The corresponding K-electrons of the $5_1^- \rightarrow 4_1^+$ transition are expected to be a factor of 3 fewer than those of the $2_2^+ \rightarrow 4_1^+$ transition. Additionally, due to the electron acceptance angle of SAGE, the energy of electrons emitted from

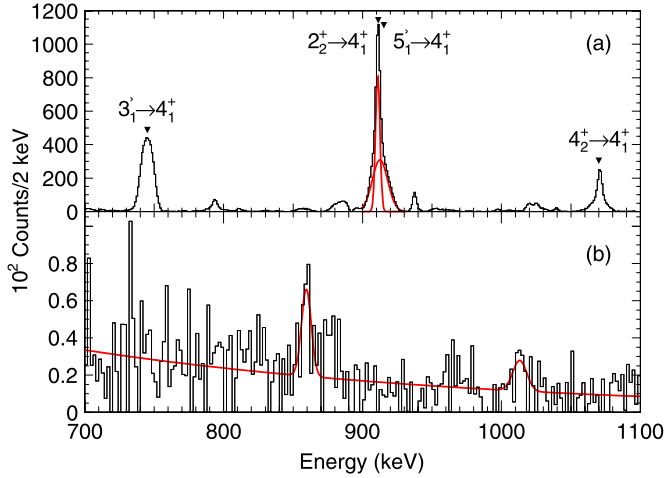


Fig. 4. (Colour online.) Spectra showing the (a) γ rays and (b) electrons detected in SAGE, both following gating on the $4_1^+ \rightarrow 2_1^+$ γ -ray transition in ^{154}Sm . Fits associated with the $2_2^+ \rightarrow 4_1^+$ γ rays and fit showing both $2_2^+ \rightarrow 4_1^+$ and $4_2^+ \rightarrow 4_1^+$ K electrons are shown. Line shapes of the $3_1^- \rightarrow 4_1^+$, $5_1^- \rightarrow 4_1^+$ and $4_2^+ \rightarrow 4_1^+$ γ rays result from the short lifetimes of the deexciting states.

the short-lived 5_1^- state will be kinematically shifted to a lower energy, ~ 845 keV. As a result the K-electrons from the $5_1^- \rightarrow 4_1^+$ transition do not interfere with the $2_2^+ \rightarrow 4_1^+$ K-electrons measurement. From the fit of the $2_2^+ \rightarrow 4_1^+$ K-electron peak at 864.1 keV, the electron peak width and centroid shift due to energy straggling and kinematic shift was established. These parameters depend on electron energy and initial state population and should then be the same for the $2_2^+ \rightarrow 2_1^+$ K-electron peak at 1049.03 keV, which is of similar energy and emitted from the same initial state.

For the $2_2^+ \rightarrow 2_1^+$ transition in ^{154}Sm , an electron peak could not be identified over the variance of the background, as shown in Fig. 5. Using a fit with the established parameters and the confidence limit formalism of Ref. [26], an upper limit for the K-electron peak was established at the 95% confidence level. Additional sources of error are quoted on top of this 95% upper limit at the 1σ level. For the ICC of the $2_2^+ \rightarrow 2_1^+$ mixed $E0 + M1 + E2$ transition in ^{154}Sm , a limit of $\alpha_K \leq 0.0067(6)$ is deduced.

For the $4_2^+ \rightarrow 4_1^+$ transition in ^{154}Sm , a small K-electron peak is observed at the expected energy, a fit to this peak is shown in Fig. 4. As electron peaks were not observed for either competing transition, strict fit constraints could not be placed on the electron peak. The electron peak area was taken at the 95% confidence level

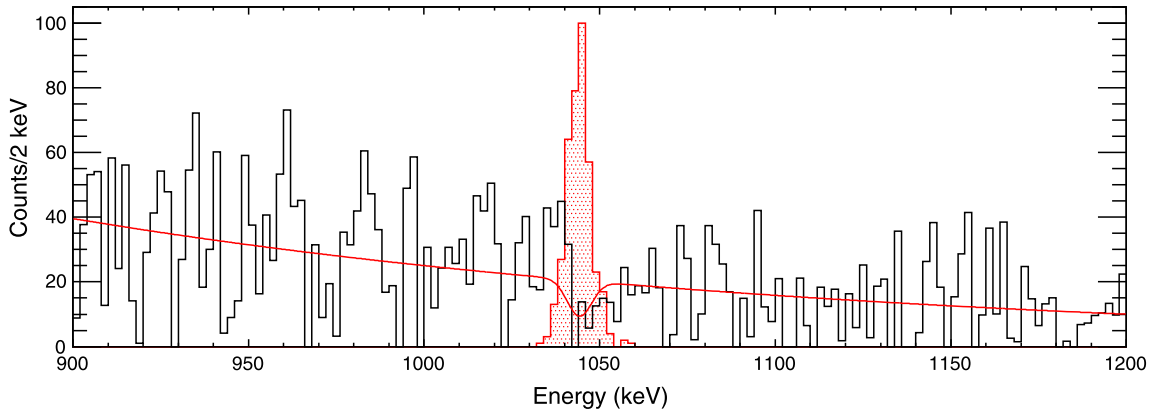


Fig. 5. (Colour online.) High-energy electron spectrum from SAGE after gating on the $2_1^+ \rightarrow 0_1^+$ γ -ray transition in ^{154}Sm . A simulated peak for the $2_2^+ \rightarrow 2_1^+$ K-electron, corresponding to $\rho^2(E0) = 100 \cdot 10^{-3}$, is overlaid. The red line shows a simple peak fit using the parameters determined from Fig. 4.

Table 2

Measured monopole transition strengths.

Nucleus	Transition	$\rho^2(E0)_{\text{exp}} \times 10^{-3}$	Literature value
^{152}Sm	$2_2^+ \rightarrow 2_1^+$	56(14)	69(6) ^a
^{154}Sm	$2_2^+ \rightarrow 2_1^+$	$\leq 9.4(15)$	< 6.3 ^b
^{154}Sm	$4_2^+ \rightarrow 4_1^+$	$8.2_{-8.2}^{+12.0}$	–

^a Value from Ref. [13].

^b Value from Ref. [21].

and a value of $\alpha_K = 0.0079_{-0.0073}^{+0.0087}$ is deduced for the for the ICC of the $4_2^+ \rightarrow 4_1^+$ mixed $E0 + M1 + E2$ transition in ^{154}Sm .

For a mixed $E0 + M1 + E2$ transition, the monopole transition strength $\rho^2(E0)$ is related to the ICC by [27]:

$$\rho^2(E0) = q_K^2(E0/E2) \cdot \frac{\alpha_K(E2)}{\Omega_K(E0)} \cdot W_\gamma(E2), \quad (3)$$

where $\alpha_K(E2)$ is the component K-electron ICC, Ω_K is an electronic factor, $W_\gamma(E2)$ is the γ -ray transition probability and the ratio $q_K^2 = W_K(E0)/W_K(E2)$ may be determined from

$$q_K^2 = \frac{\alpha_{\text{exp}}(1 + \delta^2) - \alpha_K(M1)}{\delta^2 \alpha_K(E2)} - 1. \quad (4)$$

Calculated values of $\rho^2(E0)$ from the measurements are given in Table 2, where values of δ and $W_\gamma(E2)$ for ^{154}Sm are taken from a recent measurement [11] and values of Ω_K and $\alpha_K(E2)$ are taken from the Brlcc program [25]. The ^{154}Sm $4_2^+ \rightarrow 4_1^+$ γ ray is taken to be a pure $E2$ transition, in accordance with Ref. [11], inclusion of an $M1$ component would lead to a marginally reduced $\rho^2(E0)$ value. Due to negligible γ -ray feeding from above, the $0_2^+ \rightarrow 0_1^+$ transition could not be observed in the coincidence measurements of this work.

4. Discussion

The measured $\rho^2(E0)$ values present an interesting challenge for the interpretation of the I_2^+ states. A comparison of the measured value to predictions can give useful evidence in support of, or in opposition to the models. In the case of a pure β -vibrational band, $\rho^2(E0; I_\beta^+ \rightarrow I_1^+)$ should have a value of the order of $100 \cdot 10^{-3}$. Additionally, as shown by Eq. (1), there should be no angular momentum dependence to this value. A value of $100 \cdot 10^{-3}$ is far larger than the measured $\rho^2(E0)$ values, as demonstrated in Fig. 5 where a simulated conversion electron peak of this strength is superimposed on the experimental data. Hence, it must be concluded that the states in ^{154}Sm cannot be described

as pure β vibration. Calculations performed by P. Van Isacker [16,28], in the more general collective picture of the IBM, predict $\rho^2(E0; 2_2^+ \rightarrow 2_1^+) = 39 \cdot 10^{-3}$ and $\rho^2(E0; 4_2^+ \rightarrow 4_1^+) = 31 \cdot 10^{-3}$. These values lie between those measured and β -vibrational values, but are still notably larger than the measurements presented in this work. Consequently, it must be concluded that the IBM fails to reproduce the behaviour of the 2_2^+ and 4_2^+ states, in this case, with regards to $E0$ transitions.

It should be remarked that the $\rho^2(E0; 2_2^+ \rightarrow 2_1^+)$ upper limit measured in this work agrees with the measurement in Ref. [21]. This supports the $\rho(E0; 0_2^+ \rightarrow 0_1^+) \approx 100 \cdot 10^{-3}$ value reported in Ref. [21], which was experimentally convolved with the $\rho^2(E0; 2_2^+ \rightarrow 2_1^+)$ measurement. The energy spacing of the 0_2^+ , 2_2^+ , 4_2^+ and $6_{(3)}^+$ states is indicative of a rotational band. As such, any interpretation of the nature of the 2_2^+ state as having a majority component incompatible with an interpretation of the 0_2^+ state should be approached with caution.

As the observed states of ^{154}Sm are not adequately described by the Bohr and Mottelson β vibration description or the IBM, state mixing will now be considered. In Ref. [29], it was suggested that little mixing between the GSB and 0_2^+ band should be expected. Mixing between the 0_2^+ state and 0_3^+ state, believed to be a spherical coexisting configuration, was shown to have a maximum mixing amplitude of 4%. Hence one would expect a maximum mixing amplitude of $\sim 23\%$ between the 2_2^+ and 2_3^+ states. Mixing with the 2_2^+ state at 1440 keV by a $\Delta K = 2$ coupling of the two rotational bands might also be possible. This would naturally only mix the states with $I \geq 2$ of the 0_2^+ band. Considering simple two-state mixing of the form

$$|I_2^+\rangle = \alpha |I_{\text{col}}^+\rangle + \beta |I_k^+\rangle \quad (5)$$

between a collective state I_{col}^+ , as described by either model, and another state I_k^+ with an intrinsic transition strength $\rho^2(E0; I_k^+ \rightarrow I_1^+) \approx 0$. The observed $\rho^2(E0)$ values yield upper limits of $\rho^2(E0; 2_{\text{col}}^+ \rightarrow 2_1^+) \leq 21.7 \cdot 10^{-3}$ and $\rho^2(E0; 4_{\text{col}}^+ \rightarrow 4_1^+) \leq 40.4 \cdot 10^{-3}$, which are still significantly lower than the presented collective models. It must be concluded that a different interpretation of the I_2^+ states is required, potentially a more complex sum of states with negative interference of non-zero $\hat{T}(E0)$ matrix elements.

In the IBM, the total $E0$ strength depends on the sum of many components of differing d boson number, n_d ; even small changes of admixtures from other states may decisively change the n_d distribution, reducing $E0$ strength [15]. Alternatively, it may be concluded that the small $E0$ strengths, inconsistent with either collective model, indicates that the states are largely quasi-particle in nature with little collective contribution. Such an interpretation is supported by the $B(E2; I_2^+ \rightarrow I_1^+)$ values measured in Ref. [11], which are smaller than predicted by collective models. However, this interpretation is at odds with the apparently collective $\rho^2(E0; 0_2^+ \rightarrow 0_1^+)$ measurement [21].

5. Conclusion

In this work limits for the $E0$ strengths of the $2_2^+ \rightarrow 2_1^+$ and $4_2^+ \rightarrow 4_1^+$ transitions in ^{154}Sm were measured in a coincident γ -ray and conversion electron measurement using the SAGE spectrometer. ICCs were calculated from $\gamma\gamma$ and γe^- data, which were normalised to GSB transitions of ^{152}Sm , ^{154}Sm and ^{166}Yb , following a background subtraction of time-random coincidence events. Interband ICCs in the three nuclides were measured and found to agree well with previous measurements. Values of $\rho^2(E0)$ of $\leq 9.4(15) \cdot 10^{-3}$ for the $2_2^+ \rightarrow 2_1^+$ transition and $8.2_{-8.2}^{+12.0} \cdot 10^{-3}$ for

the $4_2^+ \rightarrow 4_1^+$ transition were measured in ^{154}Sm , these are an order of magnitude smaller than expected for $I_\beta^+ \rightarrow I_{\text{GSB}}^+$ transitions. The $E0$ strength of the $2_2^+ \rightarrow 2_1^+$ transition in ^{152}Sm was also measured, and a value of $\rho^2(E0) = 56(14) \cdot 10^{-3}$ was established in agreement with previous measurements.

Acknowledgements

We thank P. Van Isacker for providing IBM predictions. This work was supported by the UK Science and Technology Facilities Council (Grant No. ST/J000124/1) and by European Nuclear Science and Applications Research (Project No. 262010). The work of beam operators and support staff at the University of Jyväskylä and Paul Morrall of STFC Daresbury is acknowledged. This work was supported by the Academy of Finland under the Finnish Centre of Excellence Programme 2006–2011 (Nuclear and Accelerator Based Physics Contract No. 213503). The authors would like to thank the GAMMAPOOL European Spectroscopy Resource for the loan of germanium detectors in JUROGAMII.

References

- [1] L. Fortunato, Solutions of the Bohr Hamiltonian, a compendium, Eur. Phys. J. A 26 (1) (2005) 1–30, <http://dx.doi.org/10.1140/epjad/i2005-07-115-8>.
- [2] P.E. Garrett, Characterization of the β vibration and 0_2^+ states in deformed nuclei, J. Phys. G 27 (2001) R1–R22, <http://dx.doi.org/10.1088/0954-3899/27/1/201>.
- [3] K. Heyde, J.L. Wood, Shape coexistence in atomic nuclei, Rev. Mod. Phys. 83 (4) (2011) 1467–1521, <http://dx.doi.org/10.1103/RevModPhys.83.1467>.
- [4] R.V. Jolos, P. von Brentano, Intrinsic frame inverse mass tensor as a function of β and γ in the Bohr Hamiltonian, Phys. At. Nucl. 75 (4) (2012) 411–419, <http://dx.doi.org/10.1134/S106377881203009X>.
- [5] N. Pietralla, O.M. Gorbachenko, Evolution of the “ β excitation” in axially symmetric transitional nuclei, Phys. Rev. C 70 (1) (2004) 011304, <http://dx.doi.org/10.1103/PhysRevC.70.011304>.
- [6] N. Blasi, et al., $E0$ decay from the first excited 0^+ state in ^{162}Yb , Phys. Rev. C 88 (2013) 014318, <http://dx.doi.org/10.1103/PhysRevC.88.014318>.
- [7] P.E. Garrett, W.D. Kulp, J.L. Wood, et al., New features of shape coexistence in ^{152}Sm , Phys. Rev. Lett. 103 (2009) 062501, <http://dx.doi.org/10.1103/PhysRevLett.103.062501>.
- [8] W.D. Kulp, J.L. Wood, P.E. Garrett, et al., Search for intrinsic collective excitations in ^{142}Sm , Phys. Rev. C 77 (6) (2008) 61301, <http://dx.doi.org/10.1103/PhysRevC.77.061301>.
- [9] S. Leshner, et al., Study of 0^+ excitations in ^{158}Gd with the $(n, n'\gamma)$ reaction, Phys. Rev. C 76 (3) (2007) 034318, <http://dx.doi.org/10.1103/PhysRevC.76.034318>.
- [10] J.F. Sharpey-Schafer, et al., A double vacuum, configuration dependent pairing and lack of β -vibrations in transitional nuclei, Nucl. Phys. A 834 (1–4) (2010) 45c–49c, <http://dx.doi.org/10.1016/j.nuclphysa.2010.01.014>.
- [11] T. Möller, N. Pietralla, et al., Absolute β -to-ground band transition strengths in ^{154}Sm , Phys. Rev. C 86 (2012) 031305, <http://dx.doi.org/10.1103/PhysRevC.86.031305>.
- [12] J.O. Rasmussen, Theory of $E0$ transitions of spheroidal nuclei, Nucl. Phys. 19 (1960) 85–93, [http://dx.doi.org/10.1016/0029-5582\(60\)90221-2](http://dx.doi.org/10.1016/0029-5582(60)90221-2).
- [13] J.L. Wood, E.F. Zganjar, C. de Coster, K. Heyde, Electric monopole transitions from low energy excitations in nuclei, Nucl. Phys. A 651 (4) (1999) 323–368, [http://dx.doi.org/10.1016/S0375-9474\(99\)00143-8](http://dx.doi.org/10.1016/S0375-9474(99)00143-8).
- [14] T. Kibedi, R.H. Spear, Electric monopole transitions between 0^+ states for nuclei throughout the periodic table, At. Data Nucl. Data Tables 89 (1) (2005) 77–100, <http://dx.doi.org/10.1016/j.adt.2004.11.002>.
- [15] P. von Brentano, et al., Alternative interpretation of sharply rising $E0$ strengths in transitional regions, Phys. Rev. Lett. 93 (2004) 152502, <http://dx.doi.org/10.1103/PhysRevLett.93.152502>.
- [16] S. Zerguine, P. Van Isacker, A. Bouldjedri, Consistent description of nuclear charge radii and electric monopole transitions, Phys. Rev. C 85 (2012) 034331, <http://dx.doi.org/10.1103/PhysRevC.85.034331>.
- [17] R.F. Casten, D. Kusnezov, N.V. Zamfir, Phase transitions in finite nuclei and the integer nucleon number problem, Phys. Rev. Lett. 82 (25) (1999) 5000–5003, <http://dx.doi.org/10.1103/PhysRevLett.82.5000>.
- [18] P.E. Garrett, W.D. Kulp, J.L. Wood, et al., Octupole and hexadecapole bands in ^{152}Sm , J. Phys. G 31 (2005) S1855, <http://dx.doi.org/10.1088/0954-3899/31/10/087>.
- [19] P. Papadakis, R.D. Herzberg, J. Pakarinen, et al., Towards combining in-beam γ -ray and conversion electron spectroscopy, AIP Conf. Proc. 1090 (1) (2009) 14–20, <http://dx.doi.org/10.1063/1.3087003>.

- [20] J. Pakarinen, P. Papadakis, J. Sorri, R.D. Herzberg, et al., The SAGE spectrometer, *Eur. Phys. J. A* 50 (53), <http://dx.doi.org/10.1140/epja/i2014-14053-6>.
- [21] K. Wimmer, R. Krücken, et al., First identification of large electric monopole strength in well-deformed rare earth nuclei, *AIP Conf. Proc.* 1090 (2009) 539–543, <http://dx.doi.org/10.1063/1.3087080>; K. Wimmer, R. Krücken, et al., [arXiv:0802.2514](https://arxiv.org/abs/0802.2514), 2009.
- [22] P. Rahkila, Grain – a java data analysis system for total data readout, *Nucl. Instrum. Methods Phys. Res., Sect. A, Accel. Spectrom. Detect. Assoc. Equip.* 595 (3) (2008) 637–642, <http://dx.doi.org/10.1016/j.nima.2008.08.039>.
- [23] J. Hamilton, A. Ramayya, et al., Experimental values of internal-conversion coefficients of nuclear transitions, *Nucl. Data. Sect. A* 1 (0) (1965) 521–602, [http://dx.doi.org/10.1016/S0550-306X\(65\)80014-3](http://dx.doi.org/10.1016/S0550-306X(65)80014-3).
- [24] M. Scheck, P.A. Butler, L.P. Gaffney, et al., Combined in-beam electron and γ -ray spectroscopy of $^{184,186}\text{Hg}$, *Phys. Rev. C* 83 (2011) 037303, <http://dx.doi.org/10.1103/PhysRevC.83.037303>.
- [25] T. Kibedi, et al., Evaluation of theoretical conversion coefficients using Brlcc, *Nucl. Instrum. Methods Phys. Res., Sect. A, Accel. Spectrom. Detect. Assoc. Equip.* 589 (2) (2008) 202–229, <http://dx.doi.org/10.1016/j.nima.2008.02.051>.
- [26] G.J. Feldman, R.D. Cousins, Unified approach to the classical statistical analysis of small signals, *Phys. Rev. D* 57 (1998) 3873–3889, <http://dx.doi.org/10.1103/PhysRevD.57.3873>.
- [27] T. Kibedi, G. Dracoulis, A. Byrne, P. Davidson, Low-spin non-yrast states and collective excitations in ^{174}Os , ^{176}Os , ^{178}Os , ^{180}Os , ^{182}Os and ^{184}Os , *Nucl. Phys. A* 567 (1) (1994) 183–236, [http://dx.doi.org/10.1016/0375-9474\(94\)90733-1](http://dx.doi.org/10.1016/0375-9474(94)90733-1).
- [28] P. Van Isacker, Nuclear charge radii and electric monopole transitions in the interacting boson model, personal communications and *AIP Conf. Proc.* 1488 (1) (2012) 45–52, <http://dx.doi.org/10.1063/1.4759381>.
- [29] R. Krücken, C.J. Barton, et al., Nature of excited 0^+ states in ^{154}Sm , *Phys. Lett. B* 454 (1999) 15–21, [http://dx.doi.org/10.1016/S0370-2693\(99\)00337-8](http://dx.doi.org/10.1016/S0370-2693(99)00337-8).